URSI - RCRS 2022, IIT (Indore), India, 1 - 4 December, 2022

Prototype Antenna feed for Observations at Decimeter and Meter Wavelengths

Shaik Sayuf*(1), C. Kathiravan(1) , G.V.S. Gireesh(1) , Indrajit V. Barve(1) and R. Ramesh(1)
(1) Indian Institute of Astrophysics, Bangalore, India; e-mail: shaik.sayuf@iiap.res.in

Abstract:

The objective of this work is to develop a prototype broadband radio antenna that can be used for observing the Sun and other astronomical sources in the 200-600 MHz band; the latter corresponds to a heliocentric height range of ~1.01-1.30 $R_\odot$ ($R_\odot$ = photospheric radius). In the case of non-solar targets, the above frequency range is well suited for the observations of Fast Radio Bursts (FRBs) and other transients. The Log Periodic Dipole Antenna (LPDA) is chosen as the feed because it has broadband, directional and uniform characteristics over its operating bandwidth as compared to other broadband antennas. Additionally, the antenna is fitted to a rotor system having minimal radio frequency interference ($\lesssim$ -100 dBm) in order to track the Sun both in hour angle and declination. It also helps to achieve uniform antenna gain as a function of frequency throughout the observing time period as compared to a stationary zenith pointing system. Although a dish antenna with a broadband feed is preferred due to a larger collecting area and better sensitivity, its gain varies appreciably over the operating bandwidth and its return loss is greater than the nominal value ($\approx$ -9.5 dB). The performance of this new system (in the standalone receiving element mode at present) is better than a dish antenna feed in terms of uniform gain and return loss over the designed operating bandwidth.

1. Introduction:

The electron number density in the Solar corona reduces from the inner to the outer corona and since the frequency of electro-magnetic wave emission from a plasma medium depends on the electron number density, the high frequency radio waves originate from the inner coronal regions and the low frequencies from the outer coronal regions. The plasma emissions in the frequency range of 200-600 MHz (0.5 meter – 1.5 meter wavelength) corresponds to the heliocentric distance range of ~1.01-1.30 $R_\odot$. Observations of the solar corona above the limb in the above distance range is one of the primary goals of the ADITYA-L1, the first Indian space solar mission. This height range is of interest since the transient energy and mass releases such as the flares, coronal mass ejections and the associated radio bursts originate there. Observations of the solar corona above the solar limb as well as on the solar disk are possible in radio observations since there is no occulting disk as like the white light coronagraphs. Also, this prospective spectral data can be combined with the spectral data obtained from existing observing systems in the 30-250 MHz band at the Gauribidanur Radio Observatory (GRO), which helps in understanding the intricate connections between the solar activities observed in decimeter and meter wavebands. In the case of non-solar targets, the 200-600 MHz frequency is well suited for observations of the Fast Radio Bursts (FRBs) and other transients. So, a prototype broadband antenna feed with a tracking system was developed for observations at the above-mentioned frequency band at the GRO. Using this new antenna system along with analog frontend receiver and Field Programmable Gate Array (FPGA) based digital backend, a two-element cross correlation based spectrograph was built.

2. Antenna development:

For the antenna element, the Log Periodic Dipole Array (LPDA) antenna was chosen as the feed because it has broadband, directional and uniform characteristics such as the gain, nearly constant impedance, Voltage Standing Wave Ratio (VSWR), radiation pattern, etc over its operating bandwidth as compared to other broadband antennas [1]. The LPDA was designed and fabricated in-house by following the works of Carrel [3] and studies carried out at GRO [4]. In order to ease the tracking operations and also to have mechanical stability, the dimensions of the LPDA were optimized to have a minimum weight with reasonable antenna gain. The antenna structure was built with Aluminum material. The design constant (τ) of the LPDA is 0.78 and the relative spacing (σ) is 0.14. The dipole length to diameter ratio was maintained around 80 and the spacing between the transmission lines of the LPDA were varied from ~2 mm at the top to ~31 mm at the bottom. After fine tuning, the maximum dimension of the LPDA was brought down to $\lesssim$1 meter and its weight is $\approx$1 kg (Figure 1). The VSWR of the antenna in the required band is below 2 which indicates the signal transmission is significant ($\gtrsim$ 90%) and the profile is shown in Figure 2. The Half-Power Beam Width (HPBW) along the E- and H-plane of the LPDA are 64° and 115° respectively and a uniform directional gain of ~7.4 dBi throughout the operating bandwidth. The effective aperture and front-to-back ratio are $0.6\lambda^2$ and

13 dB, respectively. The dimensions of the LPDA design are given in the Table 1. The radiation pattern in E-plane and in H-plane at a few frequencies within the operating bandwidth are shown in Figure 3 and Figure 4, respectively.

Table 1. Design specifications of the 200-600 MHz LPDA

Dipole number	Half dipole length (cm)	Diameter of dipole (mm)	location from feed point (cm)	Inter dipole spacing (cm)	Spacing between transmission lines of the LPDA (mm)
Top of the antenna			1		2
1	3.7	2	5	4	3.5
2	4.6	2	8	3	4
3	6.6	2	12	4	5
4	7.6	3	17	5	6.5
5	10.7	3	23	6	7.5
6	13.6	4	31	8	10
7	17.6	5	41	10	12.5
8	22.7	6	54	13	16.5
9	28.7	8	71	17	22.5
10	37.6	10	93	21	29.5
Bottom of the antenna			98	5	31

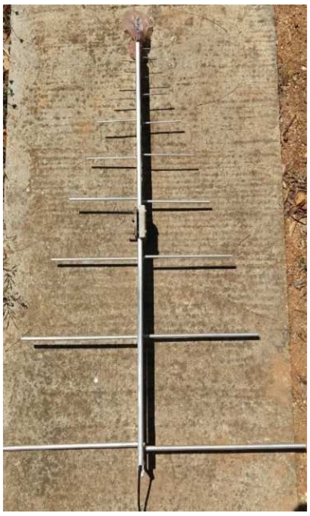

Figure 1. Photograph of the designed LPDA.

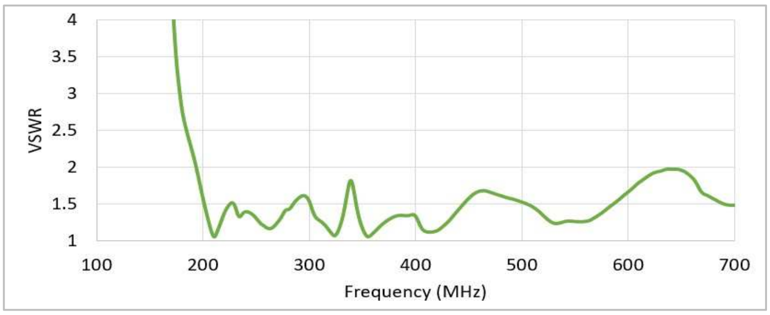

Figure 2. VSWR profile the designed LPDA.

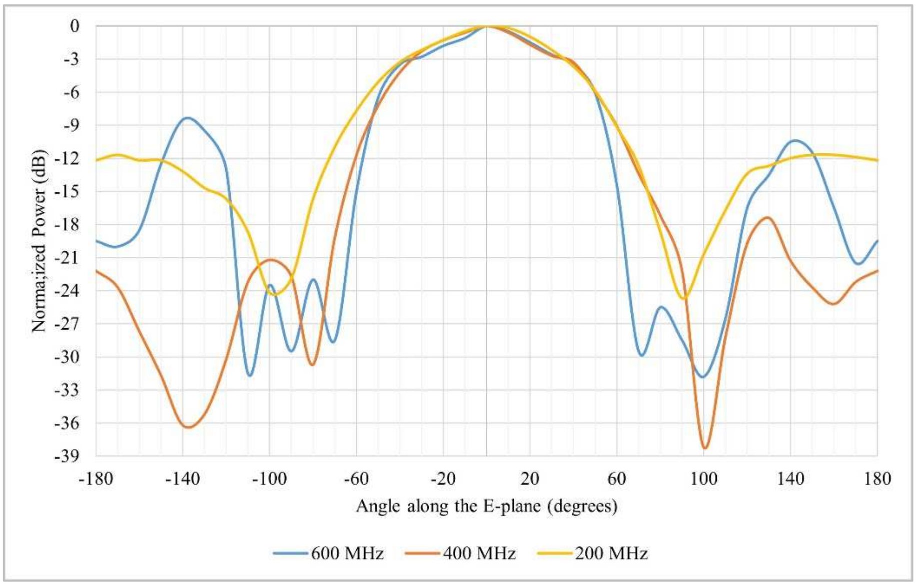

Figure 3. Radiation pattern of the designed LPDA at a few frequencies in E plane.

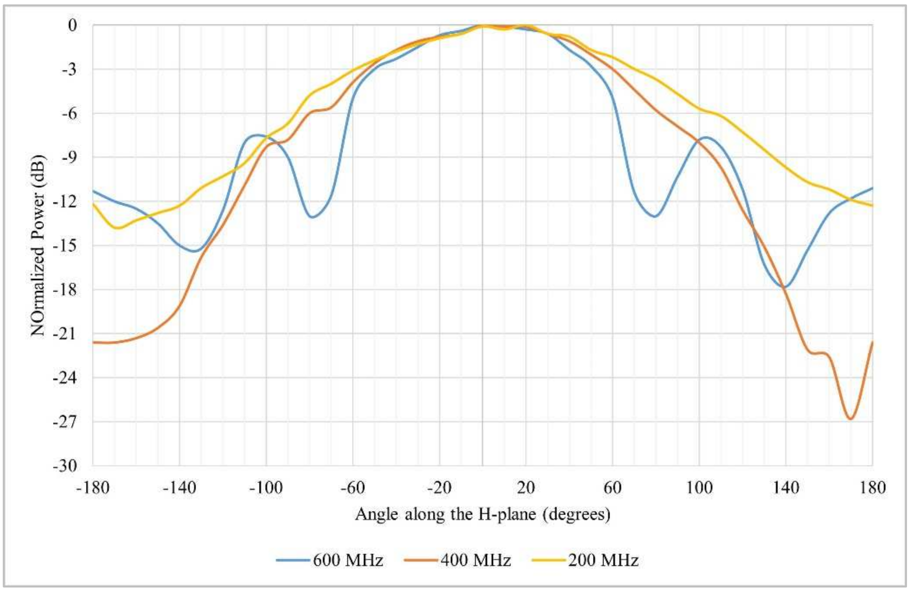

Figure 4. Radiation pattern of the designed LPDA at a few frequencies in the H-plane.

3. Tracking system:

The observed signal strength is weighted by the response pattern of the LPDA, if the antenna is kept in the stationary position and pointing towards the zenith. It helps to achieve uniform antenna gain as a function of frequency throughout the observing time period which is required to compare the solar emission at different frequencies and at different times. Also, the tracking increases the observing duration to ~9 hours. Generally, antenna systems with tracking parabolic dish reflectors are preferred at higher frequencies for larger collecting area and sensitivity. But if they have broadband antenna feeds, the gain would not be uniform throughout the operating bandwidth and also have high return loss [1]. Figure 5 shows the antenna gain variations of our LPDA and the dish antenna with tapered horn feed [1]. Figure 6 shows the corresponding return loss. Dish antenna with broadband LPDA feed also produces a non-uniform gain across the operating bandwidth and increases the return loss [2]. So, in our system, the LPDA is fitted to a rotor that allows the former to track a source with maximum gain.

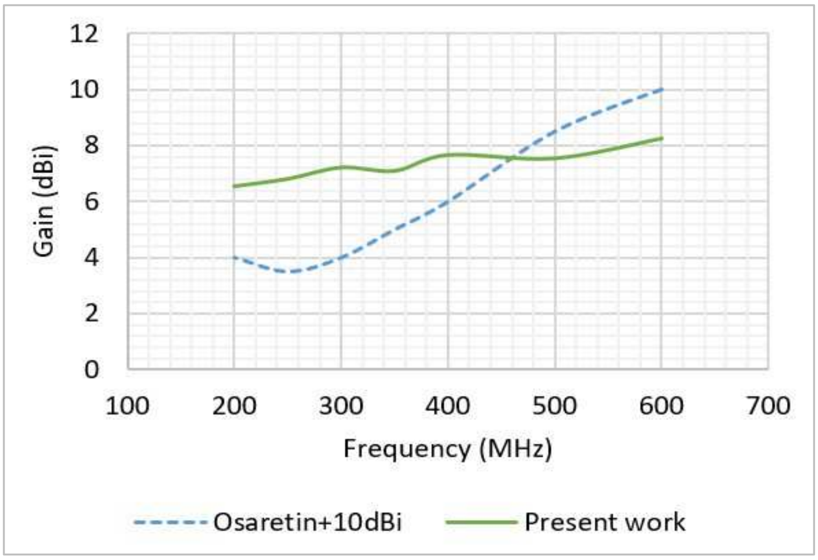

Figure 5. Antenna gain vs frequency for dish antenna system with a horn feed (Osaretin [1]) and our LPDA system. The antenna gain of the Osaretin [1] has a variation of ~7 dB whereas for the LPDA it is ~1.5 dB.

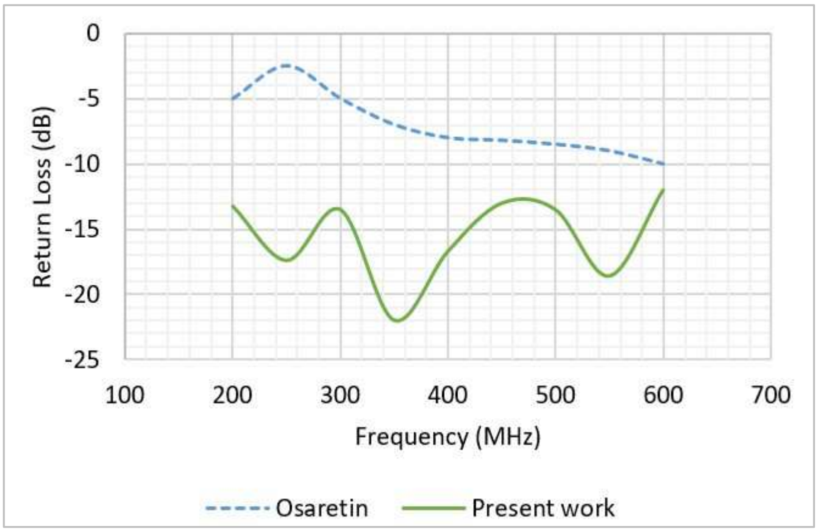

Figure 6. Return loss vs frequency of dish antenna system with a horn feed (Osaretin [1]) and our LPDA system.

The motor that is used for tracking should not produce any Radio Frequency Interference (RFI) or may produce very low RFI (≲ -90 dBm), at least within the operating band, in order to avoid the contamination of the observed astronomical data. Several commercial rotors including DiSEqC Stab HH 100 rotor and controller module [5,6] were procured, tested and found that the level of RFI generated by the latter was very low (≲ -100 dBm). This rotor can be operated over the range of -65° to +65°. The tracking speed achievable is ≈ 1°/s and it can be driven using an impulsive signal to have a fine tracking of 6′. Each rotor can handle a weight of 12 kg. The controller of the motor is commanded using a python code. Two such rotors were used for each antenna in equatorial mount; one rotor to track the source in right ascension (RA) and the other for the declination (Dec). Counter weights were also attached on either side for proper balancing of the load on the rotor. The present tracking setup is shown in Figure 7 (side view) and Figure 8 (front view). At present, these rotors do not have built-in positional encoders to get feedback on the exact pointing information of the antenna. For time domain / spectral observations this is not a serious constraint since transient emission from the corresponding sources are very intense. We are presently working on a rotor cum control system with positional feedback whose RFI generation must be lower than -120 dBm or so at any frequency in the operating bandwidth.

Figure 7. Tracking setup of the antenna (side view).

Figure 8. Tracking setup of the antenna (front view).

4. Analog and digital receiver system:

The block diagram of the receiver setup is shown in Figure 9. The signal received by the LPDA was processed initially using an analog receiver frontend. The latter has a series of radio frequency (RF) components starting from the Low-Noise Amplifier (LNA) which has a gain of ~30 dB and a noise figure (NF) of ~3 dB. Later the signal was passed through a filter section which was prepared in-house and it consists of 200-600 MHz band-pass, 250-275 MHz band-stop and 360-375 MHz band-stop filters. The 250-275MHz band-stop and 360-375MHz band-stop filters were added to remove the local RFI present in those bands mentioned. Then the signal was transmitted to receiver room using a low-loss coaxial cable. After second stage of amplification and filtering the signal in the receiver room, the 200-600 MHz RF band was converted to 50-450 MHz intermediate frequency (IF) band using an RF mixer and a local oscillator (LO at 650 MHz). The latter was then passed through a Low-Pass filter (LPF) having a cut-off of 500 MHz to supress the image frequencies.

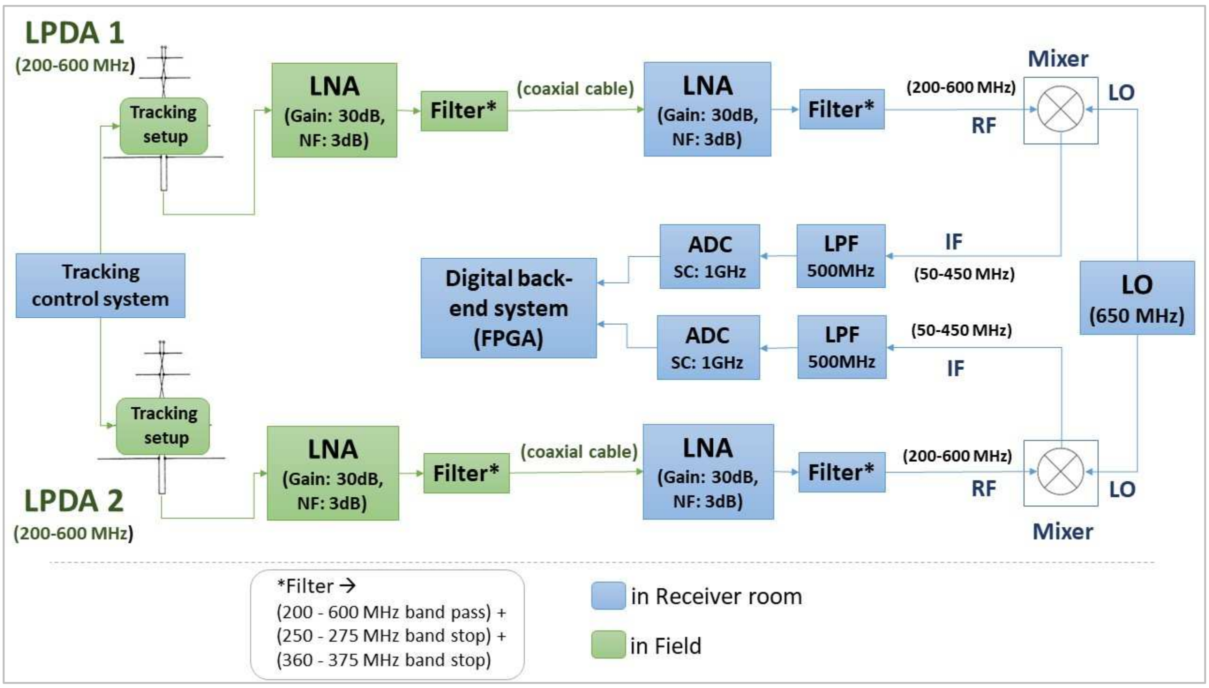

Figure 9. Block diagram of the receiver (analog + digital).

The signal was then fed into a digital receiver module; the SNAP board (Smart Network ADC Processor) developed by CASPER (Collaboration for Astronomy Signal Processing and Electronics Research) was used as a digital receiver. SNAP is a low-cost Field Programmable Gate Array (FPGA) with on board ADCs, frequency synthesizer, and two 10 Gbit Ethernet ports. It has Kintex7 system provided by Xilinx and it is operated by Raspberry pi 2 Model B processor. Photograph of the SNAP is shown in Figure 10 and the block diagram of the digital receiver is shown in Figure 11. There are 3 on-board quad Analog to Digital converters (ADC) that can work at a maximum sampling cycle (SC) of 1 GHz and therefore can handle 500 MHz band to produce an 8-bit quantized output. The digitized signal was subsequently passed through a 4-tap Poly-phase Finite Impulse Response (PF-FIR) filter having a size of 4096 and followed by a Fast Fourier Transform block (FFTB) that can produce a 1024 channel output. The PF-FIR combined with FFTB is called Polyphase Filter Bank (PFB) and the PFB based spectrometers offer vastly lowered spectral leakage over both Autocorrelation based and Fourier transform based spectrometer architectures, with a modest increase in computational requirements [7]. Here the PFB block divides the input signal into 1024 frequency bins and the 0-512 frequency bins are mirror imaged to 513-1024 bins. Effectively, the 50-450 MHz antenna signal is divided into approximately 410 frequency bins with ~1 MHz bandwidth for each bin. In the Auto-power block, the complex power of each frequency bin of PFB output was calculated for antenna 1 and antenna 2 signals individually and integrated over 1 sec, giving the auto-power spectra of each antenna signal. In the Cross-power block, the magnitude of the complex conjugate multiplication of antenna 1 and antenna 2 signals for each frequency bin was calculated and integrated over 1 sec, giving the cross-power spectra of both the antenna signals. This Digital correlation spectrometer was designed using MATLAB Simulink and programmed into the SNAP board. Though, different frequencies have different phase-centers in an LPDA feed, the delay in arrival time of these frequencies is negligible compared to the integration time of the correlator. The signal from two independent antenna systems were fed to the receiver system and the auto- and cross-power spectra were obtained simultaneously.

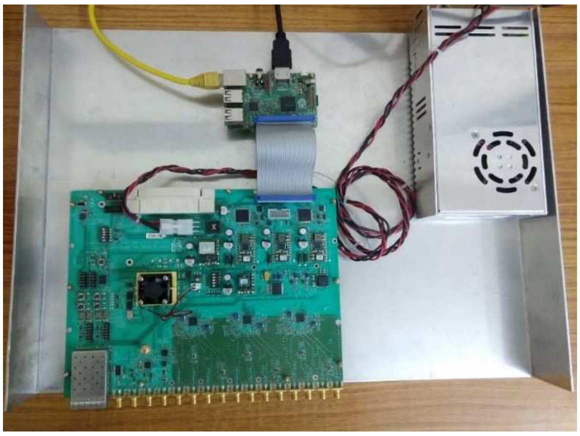

Figure 10. Photograph of SNAP board with Raspberry pi 2 Model B processor.

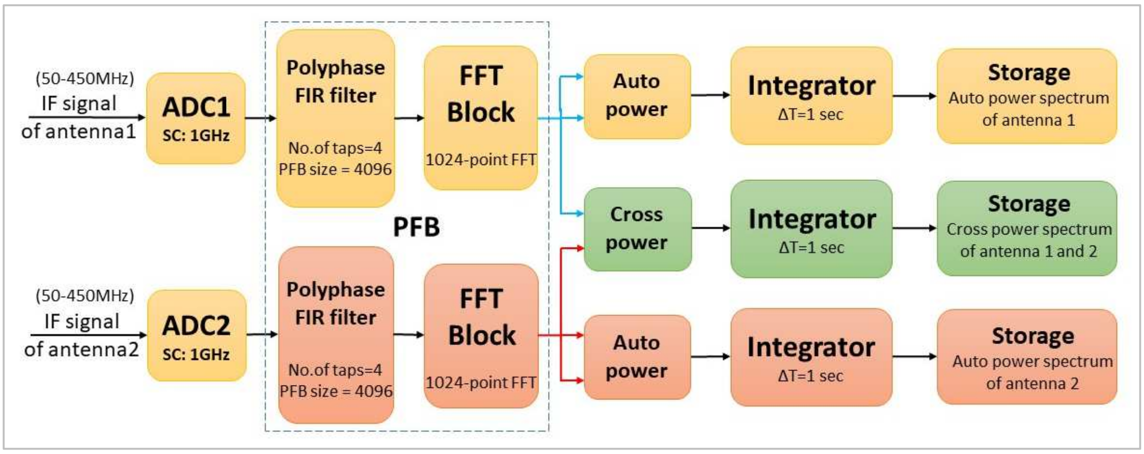

Figure 11. Block diagram of the digital receiver.

5. Observations:

The setup was kept for trial observations in the tracking mode and also in the non-tracking mode in which the LPDA was pointed towards the zenith. The baseline between the two antennas is 23 meters and was aligned in the East-West direction. At this baseline length, the sun is unresolved even at 600 MHz. The Fringes were observed when a frequency bin of 1 MHz band of one antenna signal was correlated with another antenna signal. For a frequency bin, the correlation of the signal from one antenna with in-phase signal from another antenna gives the Cosine fringe and the correlation with 90^{o} phase shifted signal from another antenna gives the Sine fringe. Square root of the sum of squares between the cosine fringe and the sine fringe gives the magnitude of the fringe which corresponds to the power of that frequency bin in the power spectrum.

Figure 12 shows the fringes observed at frequency bin 458.6 MHz on April 12, 2021 in the non-tracking mode and Figure 13 shows the fringes observed on June 26, 2021 in the tracking mode. It can be seen that in non-tracking mode; the fringes were observed for 4 hours between 5:00 UT to 9:00 UT as the HPBW of the antenna is 64^{0} in E plane. The magnitude of the fringe is maximum during sun transit time and reduces on either side of transit. Whereas, in the tracking mode, the fringes were observed with uniform maximum gain for longer durations as the antenna's maximum gain was pointing towards the Sun throughout the observation. On April 22, 2021 around 4:30 UT, a Type-III solar radio burst was detected by the antenna setup in tracking mode of observation when the Sun was very well away from the zenith. The fringes obtained at 458.6 MHz during this observation are shown in Figure 14. The burst would not have been observed if the antennas were not tracking.

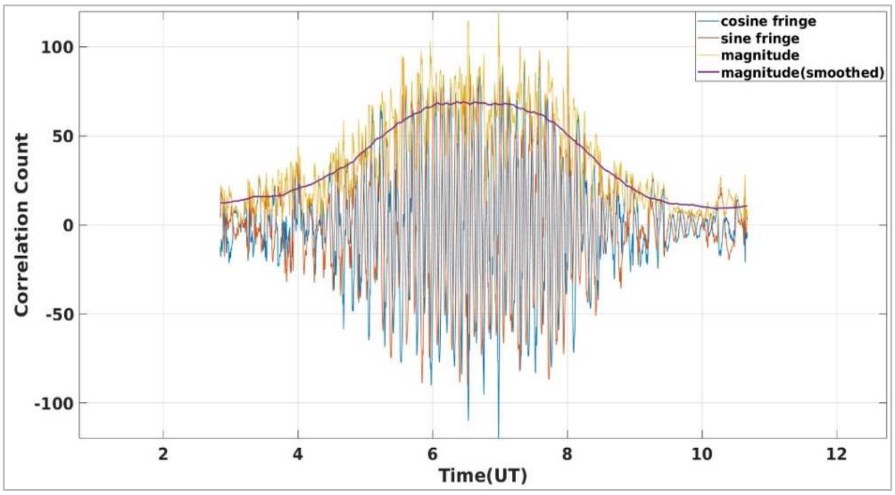

Figure 12. Fringes observed at 458.6 MHz in the non-tracking mode on April 12, 2021.

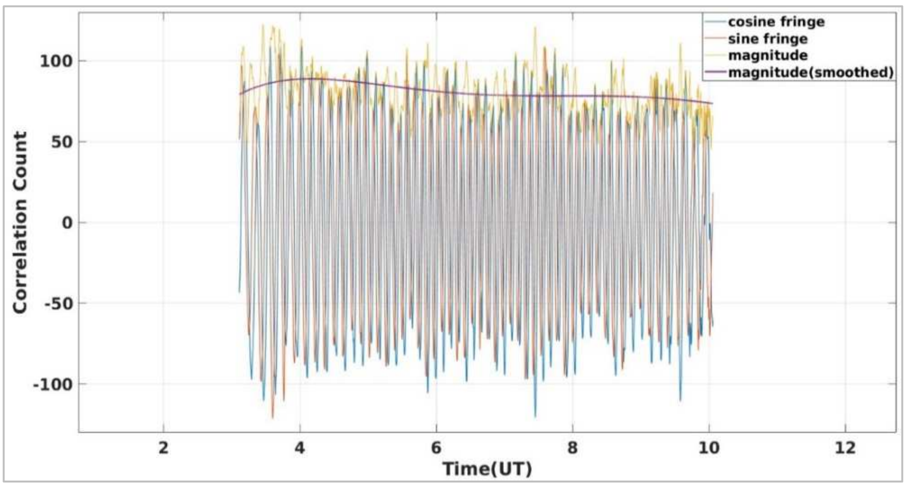

Figure 13. Fringes observed at 458.6 MHz in the tracking mode on June 26, 2021.

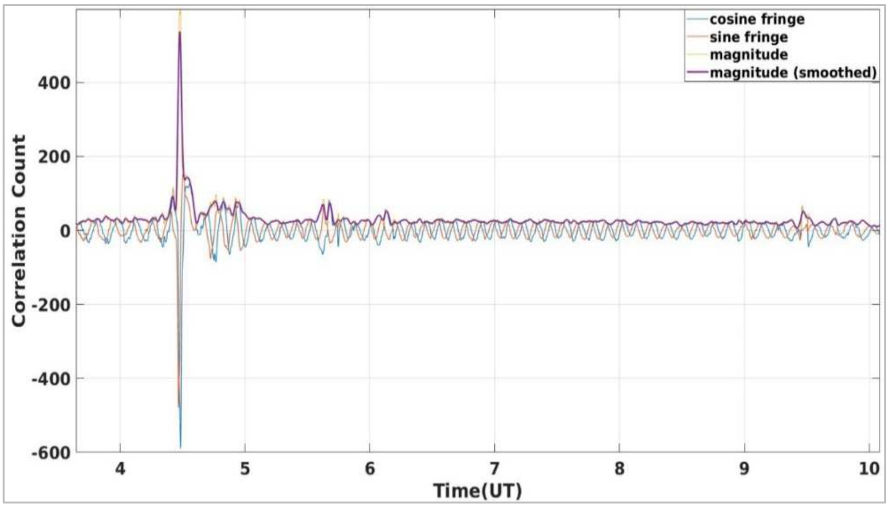

Figure 14. Fringes observed at 458.6 MHz in the tracking mode on April 22, 2021; a solar burst (a sudden increase in the correlation count) can be seen clearly above the background nearly at 4:30 UT, i.e., when the sun was away from the zenith.

6. Conclusion and future works:

A prototype tracking cross-correlation based radio spectrograph that can work in the 200-600 MHz was designed and developed at the Gauribidanur observatory. The new system has uniform gain over operating frequency as compared to a dish antenna system and has a better sensitivity than the equivalent adding interferometer system. And also, instead of tracking, if the electronic beam steering system (EBSS) were incorporated in the setup, then also the Type-III burst would not have been observed with appreciable SNR since the signal attenuation by the EBSS at high frequencies are higher as compared to low frequencies. By the virtue of correlative signal processing and tracking, we expect the new system to observe spectral signatures of relatively weak events that would be emitted by the Sun in the coming days even if its hour-angle is high. We are also considering the possibility of mounting the new LPDA on a dish antenna as a feed for observing the non-solar sources. We are also parallelly developing an indigenous rotor cum control system whose RFI generation must be as low as possible at any frequency in the operating bandwidth.

7. References:

1. I. A. Osaretin, A. Torres and C. Chen, "A Novel Compact Dual-Linear Polarized UWB Antenna for VHF/UHF Applications," in *IEEE Antennas and Wireless Propagation Letters*, January 2009, vol. 8, pp. 145-148, doi: 10.1109/LAWP.2009.2012881.

2. M. Pehlivan, K. Yeğın and Y. Aşci, "Design of 1–18 GHz parabolic reflector antenna with LPDA feed," *24th Telecommunications Forum (TELFOR)*, November 2016, pp. 1-3, doi: 10.1109/TELFOR.2016.7818833.

3. R. L. Carrell, “The Design of Log-Periodic Dipole Antennas,” *IRE International Convention Record*, March 1961, pages 61–75, volume 9.

4. Anshu kumari, “Radio polarimetric imaging of the sun corona at low radio frequencies,” *PhD thesis, Department of Applied optics and Photonics, University of Calcutta*, December 2019, chapter 3, pages 50-58.

5. “Stab HH100-HH120,” Stab Italia Instruction Manual, 2005.

6. Monstein, “Callisto DiSEqC antenna tracker,” 2018.

7. Danny C Price, “Spectrometers and Polyphase Filterbanks in Radio Astronomy”, *The WSPC Handbook of Astronomical Instrumentation, Volume 1: Radio Astronomical Instrumentation by Alex Wolszczan, World Scientific*, June 2021, p. 159-179, doi:10.1142/9789811203770_0007.